Kinetic Mechanism of Ca^{2+}-controlled Changes of Skeletal Troponin I in Psoas Myofibrils

A. J. Lopez-Davila,[†△] Fatiha Elhamine,[†△] D. F. Ruess,[†] Simon Papadopoulos,[†] Bogdan Iorga,[†‡] F. P. Kulozik,[†] Stefan Zittrich,[†] Johannes Solzin,[†] Gabriele Pfitzer,[†] and Robert Stehle[†*]

[†]Institute of Vegetative Physiology, University Cologne, Köln, Germany; and [‡]Department of Physical Chemistry, University of Bucharest, Bucharest, Romania

ABSTRACT Conformational changes in the skeletal troponin complex (sTn) induced by rapidly increasing or decreasing the [Ca^{2+}] were probed by 5-iodoacetamidofluorescein covalently bound to Cys-133 of skeletal troponin I (sTnI). Kinetics of conformational changes was determined for the isolated complex and after incorporating the complex into rabbit psoas myofibrils. Isolated and incorporated sTn exhibited biphasic Ca^{2+}-activation kinetics. Whereas the fast phase (k_{obs}~1000 s^{-1}) is only observed in this study, where kinetics were induced by Ca^{2+}, the slower phase resembles the monophasic kinetics of sTnI switching observed in another study (Brenner and Chalovich. 1999. *Biophys. J.* 77:2692–2708) that investigated the sTnI switching induced by releasing the feedback of force-generating cross-bridges on thin filament activation. Therefore, the slower conformational change likely reflects the sTnI switch that regulates force development. Modeling reveals that the fast conformational change can occur after the first Ca^{2+} ion binds to skeletal troponin C (sTnC), whereas the slower change requires Ca^{2+} binding to both regulatory sites of sTnC. Incorporating sTn into myofibrils increased the off-rate and lowered the Ca^{2+} sensitivity of sTnI switching. Comparison of switch-off kinetics with myofibril force relaxation kinetics measured in a mechanical setup indicates that sTnI switching might limit the rate of fast skeletal muscle relaxation.

INTRODUCTION

The heterotrimeric troponin complex (Tn), the tropomyosin strand (Tm), and seven actins form the regulatory unit of striated muscle thin filaments. Tn consists of the Ca^{2+}-binding subunit TnC, the inhibitory subunit TnI, and the Tm-binding subunit TnT that anchors Tn to the thin filament. The Ca^{2+}-controlled, dynamic changes of TnC, TnI, and Tm basically regulate striated muscle contraction (1,2).

Biochemical (3–10), crystal structure (11,12), NMR (13), and electron microscopy studies (14,15) have provided detailed knowledge about the structural mechanism by which Tn and Tm regulate the actomyosin interaction. Binding of Ca^{2+} to the regulatory sites on TnC induces opening of a hydrophobic patch in the N-terminal domain of TnC (N-TnC) (4) to which the switch peptide of TnI (SP-TnI) binds (16). The binding of SP-TnI to N-TnC likely exerts a drag on the neighboring inhibitory region (IR-TnI) and the C-terminal regulatory domain of troponin I (C-TnI), pulling them both off actin (9). This switching of IR-TnI and C-TnI from actin toward TnC (switch-on) not only releases the inhibitory activity of TnI itself, but also transmits the Ca^{2+} signal from TnC to Tm. When C-TnI is displaced from actin, Tm is no longer locked in a position where it blocks the transition of myosin from a weakly to a strongly bound actomyosin state (15). Following an azimuthal move of Tm on the thin filament from the outer toward the inner actin domain, cross-bridges can interact with actin in a cycling, force-generating manner: the muscle contracts (2). In reverse, relaxation is initiated by Ca^{2+} dissociating from TnC. The binding of SP-TnI to the opened state of N-TnC is no longer stabilized, thus IR-TnI and C-TnI can switch back (switch-off) and recapture their actin interactions (10). This locks Tm into its blocking position, where it prevents cross-bridge cycling (15): the muscle relaxes (2). Hence, TnI switching is a key process for muscle contraction and relaxation.

Little is known about the dynamics of Ca^{2+}-controlled TnI switching in the organized structure of the sarcomere. The Ca^{2+}-dependent kinetics of Tn were mainly explored using isolated TnC (3,5), Tn (6,8), or reconstituted thin filaments composed of actin, Tn, and Tm in the absence or presence of the soluble myosin subfragment-1 (S1), which binds strongly to actin (7,8,10,17). Pioneering studies on skeletal Tn (sTn) revealed that the assembly of sTn into reconstituted thin filaments accelerates its switch-off kinetics by an order of magnitude (8). The groups of Dong and of Davis investigated the kinetic mechanism of Ca^{2+}-controlled Tn switching using cardiac Tn (cTn) in protein systems with increasing complexity. Ca^{2+} dissociation from cTnC is slowed down by adding cTnI or cTnI + cTnT to cTnC (5,6,9,17), then accelerated when the cTn complex assembles into reconstituted thin filaments, and then slowed down again by adding S1 or S1.ADP (9,17). However, these in vitro assemblies lack the coordinated geometric arrangement and cyclic interaction between myosin and actin filaments forming the contractile machinery of the sarcomere.

Submitted March 29, 2012, and accepted for publication August 8, 2012.

[△]A. J. Lopez-Davila and Fatiha Elhamine contributed equally to this work.

*Correspondence: Robert.Stehle@Uni-Koeln.de

Editor: Malcolm Irving.

0006-3495/12/09/1254/11 $2.00

http://dx.doi.org/10.1016/j.bpj.2012.08.022

In the sarcomere, Ca^{2+}-induced switch-on kinetics of Tn have only been studied for cTn in cardiac trabeculae (18) and cardiac myofibrils (19) but not for sTn. Taken together, these studies revealed a fast conformational change associated with Ca^{2+} binding, followed by a regulatory switch. Although the switch-on of cTn is too fast to directly limit the rate of contraction (18,19), the fast reversible equilibrium between switched on and off states rate-modulates contraction (18–20). Furthermore, the intrinsic switch-off of cTn is $\approx$5 times faster than the myofibrillar force decay, making it unlikely that cTn switching directly rate-limits myocardial relaxation (19).

The findings for cardiac muscle might be not indicative for skeletal muscle. Compared to cTn, sTn possesses an additional functional Ca^{2+}-binding site (4,11,12), Ca^{2+} binding to sTn activates more actin molecules (21) and the kinetics of Ca^{2+} dissociation from isolated sTn are 2.5- to 10-fold slower (22). Incorporation of sTnC exhibiting increased or decreased Ca^{2+} dissociation rates into rabbit psoas myofibrils have been shown to speed up or slow down relaxation rates, respectively (23,24). However, because the Ca^{2+} dissociation rates were only determined for isolated sTn (24) or for sTnC in rigor myofibrils that do not contract due to the absence of the physiological substrate MgATP (22), the quantitative relation of switch-off kinetics to the rate of skeletal muscle relaxation is unknown.

Brenner and Chalovich reported a detailed study on the switch kinetics of sTnI in skinned rabbit psoas fibers (25). They did not induce sTnI switching in a forward direction by triggering Ca^{2+} binding/dissociation to/from TnC. Instead, while keeping the [Ca^{2+}] constant, they induced sTnI switching by a mechanical maneuver that rapidly releases the feedback of force-generating cross-bridges on thin filament activation. Thus, sTnI switch kinetics were induced in the backward direction via Tm on sTnI and probed by the fluorescent label *N*-((2-(iodoacetoxy)ethyl)-*N*-methyl)amino-7-nitrobenz-2-oxa-1,3-diazole (IANBD) covalently bound to sTn (sTn^{NBD}). This label mainly binds to Cys-133 on rabbit fast sTnI and changes its emission intensity according to conformational changes of sTn that perturb the environment of the label (26). Brenner and Chalovich observed monophasic fluorescence changes with rate constants k_{obs} ranging from 15 s^{-1} at low Ca^{2+} activations, up to 60–80 s^{-1} at high Ca^{2+} activations. These values were ~10- to 20-fold higher than the rate constant of force redevelopment (k_{TR}), indicating that Tm-coupled sTnI switching does not directly limit, but nevertheless does modulate the rate of contraction (25). However, the kinetics of force relaxation was not investigated in their study. Furthermore, triggering sTnI switching in the forward direction by Ca^{2+} might induce additional changes in sTnI arising from Ca^{2+} binding to sTnC that cannot be induced backward via Tm.

Here, we investigate Ca^{2+}-induced sTnI kinetics in rabbit psoas myofibrils to explore the mechanism of Ca^{2+}-controlled sTnI switching and to address the following questions: How does the incorporation of sTn into the sarcomere affect sTnI switch kinetics? How do our Ca^{2+}-induced forward kinetics of sTnI relate to the backward-induced ones in the previous study of Brenner and Chalovich (25)? Is sTnI switching a rate-limiting process for thin filament activation/inactivation? Can switch-off kinetics of sTnI limit the rate of fast skeletal muscle relaxation?

MATERIAL AND METHODS

Preparation and labeling of Tn

Rabbits (~3 kg in body weight) were sacrificed by cervical dislocation followed by exsanguination, as approved by the local animal care committee of the University of Cologne. Unlabeled Tm+sTn was prepared as described in (27) with slight modifications (see the Supporting Material).

To prepare sTn^{NBD} or sTn labeled with 5-iodoacetamidofluorescein (IAF) (sTn^{IAF}), ~1 mg/mL of Tm+sTn was reduced for 1 h at 4°C in buffer A (100 mM KCl, 1 mM EDTA, 20 mM KH_2PO_4, 2 mM DTT, pH 7.0) and dialyzed against buffer B (30 mM KCl, 10 mM imidazole, 1 mM $MgCl_2$, 1 mM EGTA, 0.02 mM DTT, pH 7.0) as in (27). IANBD or IAF (Invitrogen, Darmstadt, Germany) was added in 5- to 10-fold molar excess to Tm+sTn. The mixture was incubated for 4 h in the dark and the reaction stopped by adding 20 mM DTT. Free label was removed by dialyzing the protein 3 times for 3 h against 1 L of buffer C (1 M KCl, 5 mM KH_2PO_4, 1 mM DTT, pH 7.0). Tm was removed from sTn^{NBD}, sTn^{IAF}, or sTn by hydroxyapatite chromatography (27).

To prepare sTn selectively labeled with IAF either on sTnC ($sTn^{TnC\text{-}IAF}$) or on sTnI ($sTn^{TnI\text{-}IAF}$), sTn^{IAF} and unlabeled sTn were separated in the presence of 6 M urea into their subunits by diethylaminoethyl anion exchange and carboxymethyl cation exchange chromatography. $sTn^{TnC\text{-}IAF}$ or $sTn^{TnC\text{-}IAF}$ were reconstituted by mixing either sTnC or sTnI obtained from sTn^{IAF} with the two other subunits obtained from unlabeled sTn in 1:1:1 molar ratio, adjusting the total protein concentration to 3 mg/ml at pH 7. The complex was then formed by lowering the [KCl] in the dialysis buffer (0.5 mM $CaCl_2$, 25 mM MOPS, 1 mM DTT) first from 1 M to 0.75 M, then to 0.5 M, and finally to 0.3 M.

For storage at –80°C, labeled or unlabeled sTn were dialyzed 3 times against 1 mM NH_4HCO_3 and lyophilized.

Preparation of myofibrils and Tn exchange

After killing, the rabbit was eviscerated and placed on ice for >4 h. Thin strips (0.5 mm diameter) were dissected from the psoas muscle, pinned at their ends on a SYLGARD-coated surface and chemically skinned on ice for 2 h in rigor skinning solution (10 mM HEPES, 10 mM NaCl, 150 mM KCl, 1 mM NaN_3, 1 mM $MgCl_2$, 5 mM EGTA, 0.5%(w/v) Triton X-100, pH 7.0). The strips were then washed twice in rigor storage solution (same as rigor skinning solution but without Triton and containing in addition 0.5 mM AEBSF, 10 μM Leupeptin, 14.5 μM Antipain, and 5 μg/mL Aprotinin). Strips were stored for up to 3 days at 4°C with no detectable loss of function in stopped-flow and force measurements.

Immediately before an experiment, myofibrils were prepared by homogenizing the strips for 10 s at 4°C in the rigor storing solution using a blender at 20.000 rpm (Ultra-Turrax T25, Janke & Kunkel, Germany). The homogenate was then filtered through 44 μm polypropylene meshes to remove large bundles and the endogenous sTn exchanged by adding the exogenous sTn in $\geq$10-fold molar excess and the mixture incubated for 60 min at 20°C. The exchanged myofibrils were washed 3 times by centrifugation (5 min, 380 g, 10°C) with the buffer used in the stopped flow experiment. The myofibrils had diameters of 1–3 μm and a sarcomere length (SL) of 2.38 $\pm$ 0.07 μm (mean $\pm$ SD), which is similar to the slack SL reported for rabbit psoas myofibrils prepared under relaxing conditions (28).

Stopped-flow experiments

The Ca^{2+}-dependent fluorescence changes of isolated sTn^{IAF} and sTn^{IAF} incorporated into myofibrils (sarcomeric sTn^{IAF}) were measured at 10°C and at physiological ionic strength ($\mu = 0.17$ M). The stopped-flow apparatus (Bio-Logic SFM-400/S, Claix, France) was equipped with a TC 100/10F-cuvette (10 mm light path; dead time of 2.2 ms at 14 mL/s flow rate) or with a μFC-08-cuvette (0.8 mm light path, dead time ~250 μs at 14 mL/s). Samples were excited at 482 nm (band with ~18 nm) using a 75 W Hg-Xe-Lamp (Hamamatsu Photonics, Herrsching, Germany) coupled to a monochromator (TgK Scientific Limited, Bradford-on Avon, UK). IAF-fluorescence emission (530 nm) was monitored using a OG515 cutoff and 530/40 band pass filter.

Switch-on kinetics was induced by single-mixing (SX). To rapidly increase [Ca^{2+}] from pCa ~8 up to pCa 4.6, the isolated sTn^{IAF} or the sarcomeric sTn^{IAF} dissolved in SX-relaxing buffer (10 mM imidazole, 3 mM $MgCl_2$, 47.7 mM Na_2creatine phosphate, 1 mM ATP, 3 mM BAPTA, and 20 mM DTT, pCa > 8, pH 7, $\mu = 0.17$ M) were mixed 1:1 with SX-activating buffers (SX-relaxing buffer containing additionally variable amounts of $CaCl_2$).

Switch-off kinetics were determined by a double-mixing protocol (DX): isolated or myofibrils with incorporated sTn^{IAF} in DX-relaxing buffer (same as SX-relaxing buffer but 0.6 mM instead of 3 mM BAPTA) were first mixed 1:1 with DX-activating buffer (DX-relaxing buffer + 1.2 mM $CaCl_2$) to induce Ca^{2+} activation at pCa 5. After an aging time of 91 ms, the first mixture was mixed 1:1 with DX-inactivation-buffer (DX-relaxing buffer + 12 mM BAPTA), which rapidly (< 2 ms) decreases [Ca^{2+}] from pCa 5 to ~8.

To investigate the effect of rigor cross-bridges on the Ca^{2+}-induced switch-on and switch-off kinetics, experiments were performed as described previously, except that buffers contained 150 mM KCl but no ATP and Na_2creatine phosphate.

For switch-on and switch-off kinetics, the final concentration of isolated sTn^{IAF} was 75 μg/mL in the TC 100/10F cuvette and 300 μg/mL in the μFC-08 microcuvette. Kinetics of sarcomeric sTn^{IAF} was determined at a final myosin head concentration of 1.5 μM.

Determination of Ca^{2+} dissociation kinetics with Quin-2

6 μM sTn (or sTn^{IAF}) was dissolved in Q-buffer (10 mM Mops, 100 mM KCl, 3 mM $MgCl_2$, 1 mM DTT, pH 7) and mixed 1:1 with Q-buffer including 150 μM Quin-2 (17). No Ca^{2+} was added, because there was enough contaminating Ca^{2+} in the Q-buffer to nearly saturate the complexes. Samples were excited at 330 nm and the Ca^{2+}-dependent Quin-2 emission recorded using a 455 nm cutoff and 472/30 nm band-pass filter. To correct for sTn-unspecific changes in Quin-2 signals, background transients were recorded without sTn.

Measurement of myofibrillar force kinetics

Mechanical experiments were performed at 10°C using the same activating and relaxing buffers as for stopped-flow measurements. Briefly, skeletal myofibrils (2–5 μm in diameter, 2.1–2.3 μm in slack SL) with exchanged sTn or sTn^{IAF} were mounted in a mechanical apparatus using atomic force cantilevers for force detection, prestretched by 15% of their slack SL and rapidly (within 10 ms) Ca^{2+} activated or relaxed using a microflow solution change technique (29).

Data analysis and statistics

Fluorescence transients were corrected for Ca^{2+}-unspecific mixing artifacts by subtracting corresponding baseline transients (see Fig. S1 and description in the Supporting Material). The baseline-subtracted transients were fitted by a mono- or a biexponential function in Biokine 32 (version V4.27, Bio-Logic) and the obtained parameters analyzed in GraphPad-Prism (version 4.02). Values are given as mean ± SE.

RESULTS

Functionality of labeled sTn and its incorporation into myofibrils

We first labeled sTn with IANBD as in the studies of Brenner and co-workers (25,27). However, sTn^{NBD} incorporated into myofibrils yielded a signal/noise ratio of only ~2 (Fig. 1 *A*, *gray trace*). Labeling sTn with IAF (30) that has >3-fold higher extinction than IANBD exhibited a similar time course of fluorescence change, but a highly improved signal/noise ratio of ~10–15 (Fig. 1 *A*, *black trace*). Therefore, we used IAF-labeled sTn (sTn^{IAF}).

To test whether labeling with IAF affects the kinetics of Ca^{2+} dissociation from isolated sTn, Ca^{2+}-saturated sTn or Ca^{2+}-saturated sTn^{IAF} was mixed with the Ca^{2+} indicator Quin-2 (Fig. 1 *B*). Single exponential fitting of the transients yielded no significant differences in rate constants (unlabeled sTn: 3.3 ± 0.5 s^{-1}; $n = 5$; labeled sTn^{IAF}: 3.6 ± 0.6 s^{-1}; $n = 5$). Furthermore, no significant differences in kinetic parameters of Ca^{2+}-induced force development and relaxation were found between myofibrils exchanged with unlabeled sTn or sTn^{IAF} (see Table S1 in the Supporting Material). These controls indicate that labeling of sTn does not alter the kinetic and regulatory properties of sTn.

A prerequisite for determining sTn^{IAF}-kinetics in the sarcomere is that sTn^{IAF} binds specifically to the thin filament. After exchanging the endogenous sTn by sTn^{IAF} under rigor conditions, the IAF fluorescence localized in the filament overlap region where the rigor cross-bridges activate the thin filament (Fig. 1, *C–E*). Control experiments performed at longer SLs verified that the sTn^{IAF} is not bound in the center of the sarcomere. This excludes unspecific binding of sTn^{IAF} to myosin filaments (Fig. 1, *D* and *E*). These findings are in agreement with previous studies (27,31,32).

Switch-on kinetics of sTn^{IAF} induced by high [Ca^{2+}]

Isolated sTn^{IAF} or sTn^{IAF} incorporated into myofibrils (sarcomeric sTn^{IAF}) were mixed with activating buffer to rapidly increase [Ca^{2+}] from pCa ~8 to 4.6 (25 μM Ca^{2+}). The baseline-subtracted transients exhibited biphasic fluorescence changes that were fitted by double exponential functions (Fig. 2, *A* and *B*), to obtain the rate constants $k_{obs(fast)}{}^{+Ca}$ and $k_{obs(slow)}{}^{+Ca}$ and the relative amplitudes A_{fast} and A_{slow} listed in Table 1. To accurately measure the fast process with isolated sTn^{IAF} we had to use a small μ-cuvette with a very short dead time of 0.25 ms (Fig. 2 *A*). Due to the higher viscosity of the myofibrillar samples, only the standard cuvette providing a dead time of 2.2 ms could be used

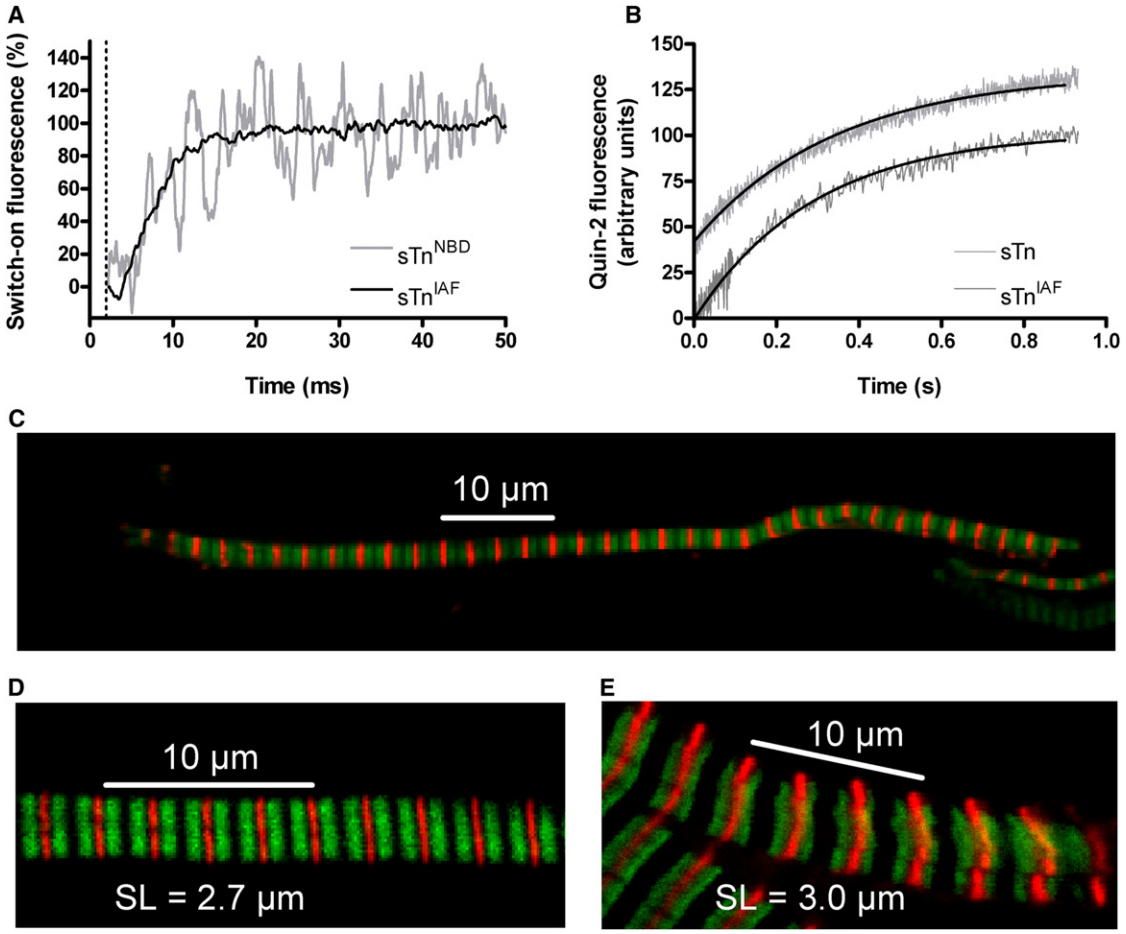

FIGURE 1 Effect of labeling on the kinetics of sTn and incorporation into the sarcomere. (*A*) Effect of changing the label on kinetics. Myofibrils having incorporated either sTn^{IAF} or sTn^{NBD} are mixed at time = 0 with high [Ca^{2+}] (pCa 4.6). (*B*) Effect of IAF labeling on the kinetics of Ca^{2+} dissociation from isolated sTn probed by Quin-2 fluorescence. (*C–E*) Localization of sTn^{IAF} in the sarcomere resolved by confocal microscopy. Green: sTn^{IAF} emission, red: Z discs marked with Alexa 532/anti-α-actinin.

for sarcomeric sTn^{IAF}. However, incorporation of sTn^{IAF} inverted the polarity of the fast phase, which facilitated the differentiation of two phases (Fig. 2 *B*). Despite the changed polarity, the values of $k_{obs(fast)}{}^{+Ca}$ and $k_{obs(slow)}{}^{+Ca}$ for sarcomeric sTn^{IAF} did not significantly differ from those measured for isolated sTn^{IAF} (Table 1).

To investigate switch-on kinetics of sarcomeric sTn^{IAF} in the presence of strongly bound rigor cross-bridges, [Ca^{2+}] was increased from pCa ~8 to 4.6 in the absence of ATP. The baseline-subtracted transients can be fitted by monoexponentials, yielding a k_{obs} of 142 ± 35 s^{-1} ($n = 6$), which is not significantly different from $k_{obs(slow)}{}^{+Ca}$ of 152 ± 19 s^{-1} ($n = 7$) obtained in the presence of MgATP (Table 1). Thus, rigor cross-bridges do not accelerate the switch-on of sTn^{IAF} induced by high [Ca^{2+}].

Origin of Ca^{2+}-induced changes of sarcomeric sTn^{IAF}

So far, we had labeled the whole rabbit sTn complex as in previous studies (25,30). However, the three fast sTn subunits of rabbit contain four potential labeling sites, i.e., four cysteines: C98 on sTnC, and C48, C64, and C133 on sTnI (none on sTnT). Nevertheless, Greene (30) reported that IAF exclusively labels sTnI. To verify this, the three sTn subunits were separated by SDS-PAGE and the gel excited under ultraviolet light (Fig. 2 *C*), which revealed that some IAF was also bound to sTnC. To test whether the biphasic fluorescence change originates from structural changes in two distinct subunits (e.g., the fast change from sTnC and the slow change from sTnI), sTn was separated into its three subunits. sTnC or sTnI was then selectively labeled with IAF and reconstituted into heterotrimeric complexes consisting of selectively labeled TnC ($sTn^{TnC\text{-}IAF}$) or selectively labeled sTnI ($sTn^{TnI\text{-}IAF}$). Although Ca^{2+} induced no detectable fluorescence change in $sTn^{TnC\text{-}IAF}$ in myofibrils (Fig. 2 *D*, *black transient*), $sTn^{TnI\text{-}IAF}$ in myofibrils (= sarcomeric $sTn^{TnI\text{-}IAF}$; Fig. 2 *D*, *gray transient*) yielded a biphasic fluorescence transient similar to that obtained when labeling the complex as a whole (sarcomeric sTn^{IAF}; see transient in Fig. 2 *B*). The fast phase of sarcomeric $sTn^{TnI\text{-}IAF}$ was also observed

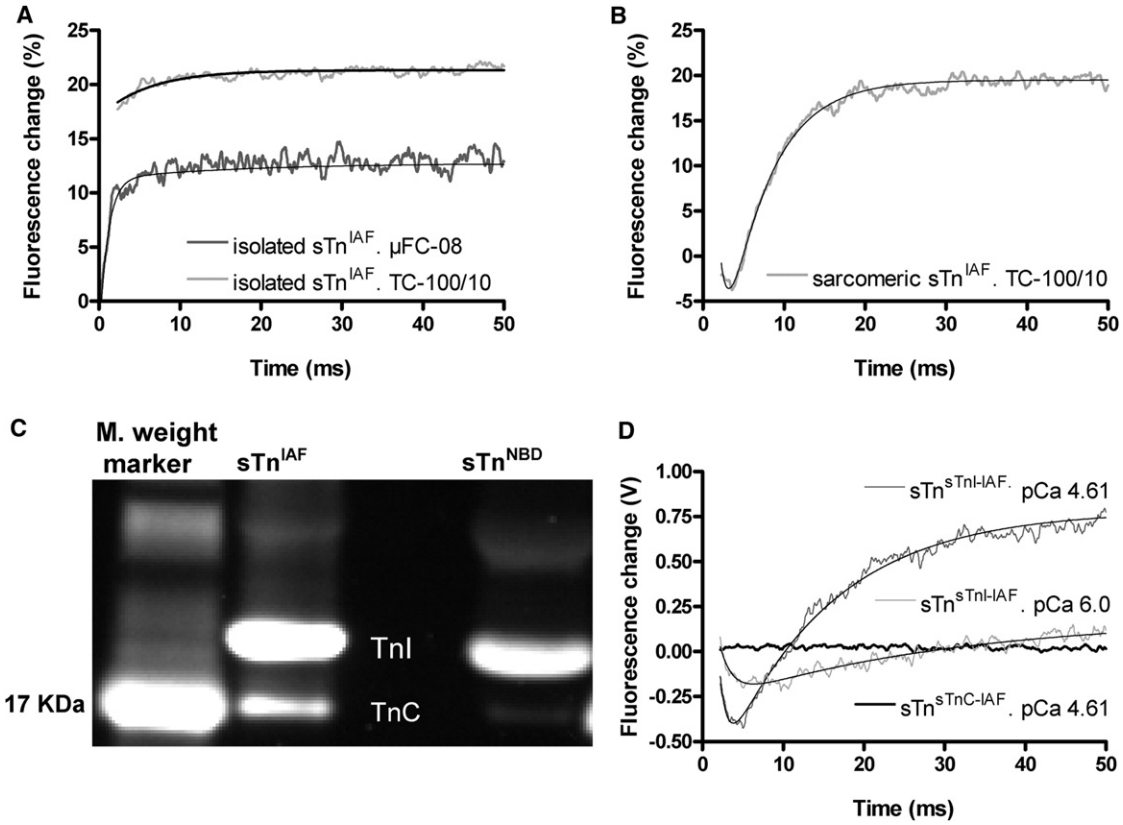

FIGURE 2 Biphasic kinetics of sTn^{IAF} following a rise in $[Ca^{2+}]$ and the origin of fluorescence changes. (*A*) Percental fluorescence changes upon mixing isolated sTn^{IAF} with high $[Ca^{2+}]$ in the standard and microcuvette, both mixings resulting in pCa 4.6. (*B*) As in *A* for sarcomeric sTn^{IAF} (only standard cuvette). (*C*) sTnT, sTnI, and sTnC subunits from 100 μg sTn^{IAF} and 100 μg sTn^{NBD} are separated on a 10–20% SDS-polyacrylamide gel (Tris-Tricine) and IAF-fluorescence excited by ultraviolet light. (*D*) Fluorescence transients of myofibrils with incorporated IAF-labeled sTn complexes that have been selectively labeled either on TnC ($sTn^{TnC\text{-}IAF}$) or on TnI ($sTn^{TnI\text{-}IAF}$).

upon changing from pCa ~8 to lower $[Ca^{2+}]$ (pCa 6) (Fig. 2 *D*, *light gray transient*). At pCa 6, the kinetics of both phases was slower than at high $[Ca^{2+}]$ (see Table 1). These findings indicate that the biphasic kinetics derive from Ca^{2+}-induced kinetics probed by IAF bound to sTnI.

Interestingly, a lower value of $k_{obs(slow)}{}^{+Ca}$ was obtained with sarcomeric $sTn^{TnI\text{-}IAF}$ ($88 \pm 5\ s^{-1}$ at pCa 4.6) than with sarcomeric sTn^{IAF} ($152 \pm 19\ s^{-1}$) (Table 1). This might reflect lower protein activity due to the urea denaturation required to dissolve the sTn subunits. Therefore, all further experiments were performed using sTn^{IAF}, avoiding the denaturation and renaturation required for subunit separation and complex reconstitution. To identify the labeled sites, sTnI was purified from sTn^{IAF} and partially digested. Mapping the peptides by mass spectroscopy revealed that IAF is only covalently bound to peptides containing C133,

TABLE 1 Relative amplitudes and rate constants of Ca^{2+}-induced fluorescence changes

			Fast phase		Slow phase	
Preparation	pCa	*n*	A_{fast} (%) *	$k_{obs(fast)}{}^{+Ca}$ (s^{-1})	A_{slow} (%) *	$k_{obs(slow)}{}^{+Ca}$ (s^{-1})
Isolated sTn^{NBD}	4.6	4	8.0 ± 1.2	1283 ± 86	1.5 ± 0.3	134 ± 11
Sarcomeric sTn^{NBD}	4.6	9	n.d.	n.d.	9.2 ± 0.9	131 ± 15
Isolated sTn^{IAF}	4.6	5	8.8 ± 1.2	1053 ± 134	1.9 ± 0.2	131 ± 20
Sarcomeric sTn^{IAF}	4.6	7	13.1 ± 1.4	1068 ± 104	35.2 ± 3.3	152 ± 19
Sarcomeric sTn^{IAF}, rigor	4.6	6	–	–	12.0 ± 2.0	142 ± 35
Sarcomeric $sTn^{TnI\text{-}IAF}$	4.6	8	9.4 ± 1.2	900 ± 193	24.5 ± 1.3	88 ± 5
Sarcomeric sTn^{NBD}	6.0	5	n.d.	n.d.	4.6 ± 0.6	28 ± 9
Sarcomeric sTn^{IAF}	6.0	5	6.6 ± 0.7	248 ± 37	14.9 ± 1.6	26 ± 5
Sarcomeric $sTn^{TnI\text{-}IAF}$	6.0	7	4.8 ± 0.6	247 ± 7	9.8 ± 1.2	22 ± 1

sTn^{NBD} and sTn^{IAF} was prepared by labeling whole complexes, $sTn^{TnI\text{-}IAF}$ by selective labeling of sTnI. Values present mean ± SE of *n* experiments.
*Amplitudes of Ca^{2+}-induced fluorescence changes are expressed as percentage of the initial fluorescence at pCa > 8.

and not to peptides containing C48 or C64 (Table S2). Hence, although the whole complex is labeled, our results indicate that the biphasic transient originates exclusively from C133 on sTnI. The fact that single sites and single donor-acceptor pairs can probe two conformational changes of Tn concurs with previous findings for cTn (6,10,19).

Ca^{2+} dependence of the switch-on of sTn^{IAF}

The relationship between Ca^{2+}-induced changes in isolated sTn^{IAF} and sarcomeric sTn^{IAF} and activating [Ca^{2+}] are summarized in Fig. 3. Exponential functions were fitted to the baseline-subtracted fluorescence transients of isolated sTn^{IAF} (Fig. 3 *A*) and sarcomeric sTn^{IAF} (Fig. 3 *B*; for original and baseline transients see Fig. S1 *C*). The amplitudes (Fig. 3, *D* and *E*), and rate constants (Fig. 3, *F* and *G*), obtained from the fits were plotted against the pCa and fitted by sigmoidal Hill functions to derive the Ca^{2+} sensitivity (pCa_{50}-value), the cooperativity (*nH*-value), the maximum value at high [Ca^{2+}], and, for rate constants, also their minimum value at low [Ca^{2+}]. The corresponding values obtained from fitting the Hill function to the parameter-pCa relationships derived from individual experiments are listed in Table 2.

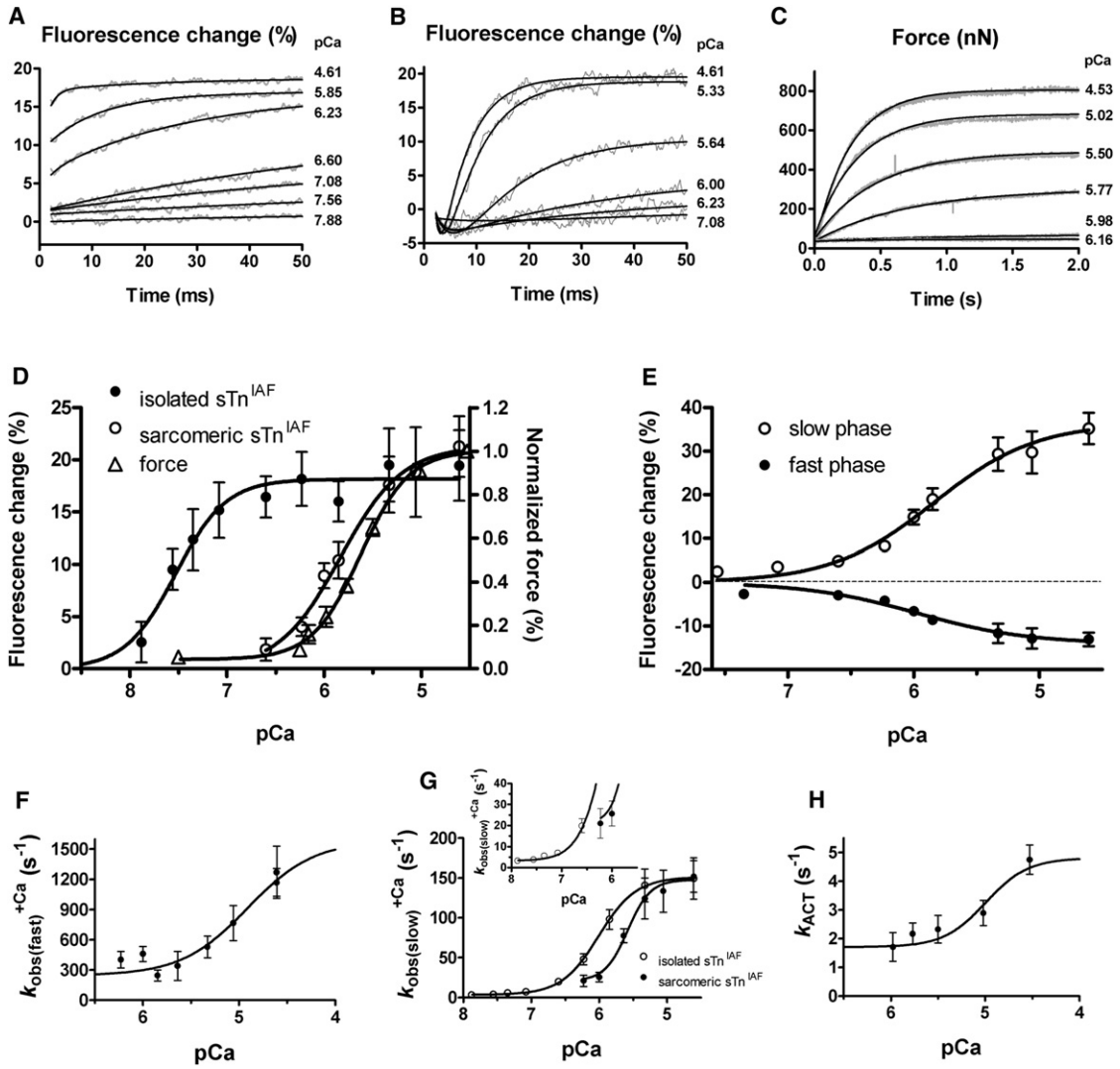

FIGURE 3 Ca^{2+} dependence of sTn^{IAF} switch-on and its relation to force-development kinetics. (*A*) Fluorescence transients following mixing isolated sTn^{IAF} with increasing [Ca^{2+}]. (*B*) As in *A* but for sarcomeric sTn^{IAF}. (*C*) Kinetics of Ca^{2+}-induced force development of myofibrils with incorporated sTn^{IAF}. (*D*) Ca^{2+} dependence of total fluorescence changes in isolated and sarcomeric sTn^{IAF} in relation to force. (*E*) Ca^{2+} dependence of the fluorescence amplitudes of the fast (*negative*) and slow (*positive*) phase of sarcomeric sTn^{IAF}. (*F*) Ca^{2+} dependence of the rate constants of the fast phase of sarcomeric sTn^{IAF}. (*G*) Ca^{2+} dependence of the rate constants of the slow phase of isolated and sarcomeric sTn^{IAF}. (*H*) Ca^{2+} dependence of the rate constant of Ca^{2+}-induced force development. Note, Hill curves in *D–H* represent a single fit to the means pooled from all experiments and might deviate slightly from the Hill parameters listed in Table 2 obtained from fitting Hill curves to individual experiments.

TABLE 2 Ca^{2+} dependence of sTn^{IAF} fluorescence and force parameters

Preparation	Parameter	*	*N*	pCa_{50}	*nH*	Min. value	Max. value
	Fluorescence						
Isolated sTn^{IAF}	Total amplitude	3 D	5	7.50 ± 0.08	2.4 ± 0.6	–	19.4 ± 3.1%
	$k_{obs(slow)}{}^{+Ca}$	3 G	6	6.04 ± 0.07	2.0 ± 0.3	3.2 ± 0.4 s^{-1}	152 ± 23 s^{-1}
Myofibrils.sTn^{IAF}	Total amplitude	3 D	5	5.98 ± 0.11	2.4 ± 0.3	–	21.3 ± 2.7%
	Fast amplitude	3 E	8	5.95 ± 0.14	1.3 ± 0.3	–	−13.1 ± 1.4%
	$k_{obs(fast)}{}^{+Ca}$	3 F	4	4.90 ± 0.20	1.3 ± 0.4	244 ± 37 s^{-1}	1580 ± 90 s^{-1}
	Slow amplitude	3 E	7	5.96 ± 0.09	1.8 ± 0.3	–	35.2 ± 3.3%
	$k_{obs(slow)}{}^{+Ca}$	3 G	4	5.50 ± 0.16	2.1 ± 0.5	21 ± 6 s^{-1}	152 ± 25 s^{-1}
	Force						
Myofibrils.sTn^{IAF}	Amplitude	3 D	16	5.66 ± 0.06	2.2 ± 0.2	5.4 ± 0.5 nN/μm^2	115 ± 14 nN/μm^2
	k_{ACT}	3 H	8	5.00 ± 0.12	1.9 ± 0.6	1.6 ± 0.4 s^{-1}	4.8 ± 0.8 s^{-1}
Myofibrils.sTn†	Amplitude		3	5.78 ± 0.09	2.2 ± 0.2	4.7 ± 1.2 nN/μm^2	134 ± 18 nN/μm^2
Myofibrils	Amplitude		8	5.83 ± 0.05	2.8 ± 0.4	5.0 ± 0.7 nN/μm^2	169 ± 15 nN/μm^2

*Reference to Fig. 3. Values present mean ± SE derived from fitting Hill curves to the data sets of *n* individual experiments.
†Myofibrils reconstituted with exogeneous unlabeled sTn.

Ca^{2+} sensitivity of sTn switching is dramatically reduced after incorporating sTn^{IAF} into the sarcomere (Fig. 3 *D* and Table 2). The pCa_{50}-value for the total fluorescence change is shifted by 1.5 units; in other words, to induce the half-maximal change, 30-fold higher [Ca^{2+}] is required for sarcomeric sTn^{IAF} compared to isolated sTn^{IAF}. The Ca^{2+} dependence values of the individual amplitudes of the fast and slow phase of sarcomeric sTn^{IAF} are plotted in Fig. 3 *E*. The pCa_{50} and *nH*-values of the two phases are very similar (Table 2).

The Ca^{2+}-dependent kinetics of the fast phase yields a minimum value of 244 ± 37 s^{-1} ($n = 4$) for sarcomeric sTn^{IAF} ($k_{obs(fast)}{}^{+Ca}$ in Fig. 3 *F*). This value reflects the reverse transition of the fast process when the forward kinetics promoted by Ca^{2+} binding become negligible. Whereas at high [Ca^{2+}], the kinetics of the slow phase of sarcomeric sTn^{IAF} are similar to those of isolated sTn^{IAF} (Fig. 3 *G* and maximum values of $k_{obs(slow)}{}^{+Ca}$ in Table 2), the minimum values of $k_{obs(slow)}{}^{+Ca}$ at low [Ca^{2+}] differ by a factor of 7 (Fig. 3 *G*, *inset* and Table 2). Because at low [Ca^{2+}], Ca^{2+} binding and contribution of the on-rate to $k_{obs(slow)}{}^{+Ca}$ become negligible, this result indicates that incorporating sTn^{IAF} into the sarcomere increases the off-rate ~7-fold.

Ca^{2+}-dependent force development kinetics of myofibrils with incorporated sTn^{IAF}

Ca^{2+}-induced myofibrillar force transients were recorded in a mechanical setup using atomic force cantilevers (29). In this setup, [Ca^{2+}] changes rapidly (within ~10 ms) from low to high concentrations, or vice versa. The observed force kinetics following a step increase of [Ca^{2+}] are consistent with previous reports for rabbit psoas myofibrils (28,33), revealing a monoexponential rise of force (Fig. 3 *C*) with a rate constant k_{ACT} that increases with increasing [Ca^{2+}] to a value of 4.7 ± 0.6 s^{-1} at pCa 4.6 ($n = 17$) (Fig. 3 *H*; Table 2). The relationships of the force and k_{ACT} to the pCa are illustrated in Fig. 3, *D* and *H*. The mean ± SE of the pCa_{50} and *nH* were obtained by fitting the sigmoidal Hill function to the corresponding relationships from individual experiments (Table 2). The force-pCa relationship is similar to the fluorescence-pCa relationship of sarcomeric sTn^{IAF} but very different from the relationship of isolated sTn^{IAF} (Fig. 3 *D* and Table 2). This confirms that the sarcomeric sTn^{IAF} signal, but not the isolated sTn^{IAF} signal can reflect the Ca^{2+}-dependent switch of sTnI regulating force development, i.e., the regulatory switch. Comparing Fig. 3 *H* with Fig. 3 *G* shows that at all [Ca^{2+}], $k_{obs(slow)}{}^{+Ca}$ is ~20-fold higher than k_{ACT}. This indicates that the Ca^{2+}-induced structural changes of sTn occur ~20 times faster than cross-bridges enter force-generating states.

Switch-off of sTn^{IAF} and force relaxation

To explore the effect of incorporation on the switch-off of sTn, isolated sTn^{IAF} or sarcomeric sTn^{IAF} was first Ca^{2+} activated for 91 ms at pCa 5, and then inactivated by switching to pCa 8. With isolated sTn^{IAF}, inactivation induced a slow fluorescence decay that was fitted by a monoexponential function (Fig. 4 *A*) yielding $k_{obs(slow)}{}^{-Ca}$ of 1.5 ± 0.2 s^{-1} ($n = 6$). With sarcomeric sTn^{IAF} (Fig. 4 *A*), inactivation started with a fast increase followed by a slower fluorescence decay. The fast increase mirrors the fast decrease observed in the switch-on experiments, and therefore represents the reversal rate of the fast process. In line with this interpretation, the observed rate constant $k_{obs(fast)}{}^{-Ca}$ of 253 ± 70 s^{-1} ($n = 5$) is similar to the minimum $k_{obs(fast)}{}^{+Ca}$ value of 244 ± 37 s^{-1} at low [Ca^{2+}] in Table 2. The major fluorescence decay that represents the switch-off is 8 times faster for sarcomeric sTn^{IAF} ($k_{obs(slow)}{}^{-Ca}$ = 11.9 ± 0.5 s^{-1}; $n = 6$) than for the isolated sTn^{IAF}. This eightfold increase in $k_{obs(slow)}{}^{-Ca}$ corresponds to the sevenfold increase in $k_{obs(slow)}{}^{+Ca}$ observed at low [Ca^{2+}]

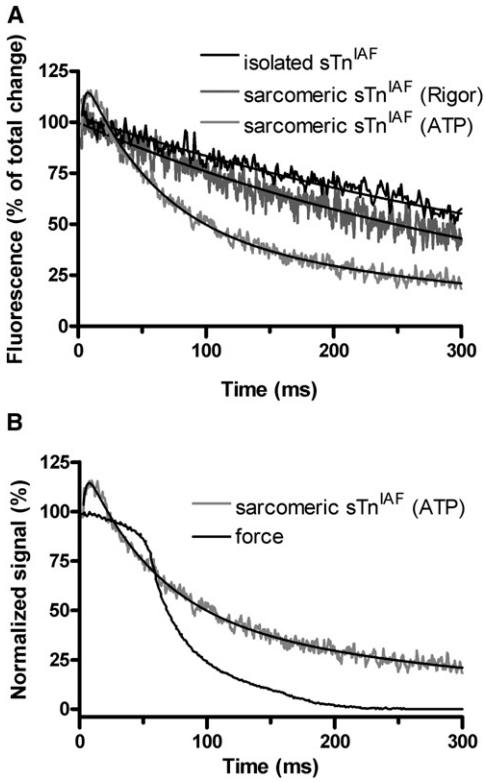

FIGURE 4 Kinetics of Ca^{2+}-induced switch-off of sTn^{IAF} and its relation to force relaxation. (*A*) Normalized fluorescence changes upon mixing Ca^{2+}-activated, isolated sTn^{IAF}, or Ca^{2+}-activated sarcomeric sTn^{IAF} ± ATP with the rapid Ca^{2+}-chelator BAPTA. Note the biphasic transient with sarcomeric sTn^{IAF} + ATP. (*B*) Fluorescence changes in sarcomeric sTn^{IAF} (as in *A*) compared to the biphasic kinetics of force relaxation. Although the initial slow linear phase of the force decay lasts longer than the fast fluorescence increase of sarcomeric sTn^{IAF} + ATP, the subsequent slow phases exhibit similar kinetics.

(Table 2). Both results indicate that incorporation speeds up the switch-off of sTnI.

To compare the switch-off with myofibrillar relaxation, force decay kinetics following rapid reduction of $[Ca^{2+}]$ from pCa 4.6 to 8 were measured in the mechanical setup (Fig. 4 *B*). The force decay is biphasic, as reported previously (28); it starts with a slow, linear decay with a rate constant k_{LIN} of 1.9 ± 0.6 s^{-1} ($n = 16$) lasting for time $t_{LIN} = 0.051 \pm 0.006$ s ($n = 16$) until sarcomeres rapidly elongate (29), at which point force decays rapidly and exponentially with the rate constant $k_{REL} = 21.1 \pm 1.5\ s^{-1}$ ($n = 16$). Noteworthy, in the stopped flow experiments where myofibrils contract without external load, the $k_{obs(slow)}{}^{-Ca}$ determined is even slightly lower than the k_{REL} measured in the setup where the myofibrils generate force. Thus, even without feedback from force-generating cross-bridges, the switch-off of sTn could be a rate-limiting step for fast skeletal muscle relaxation.

Furthermore, $k_{obs(slow)}{}^{-Ca}$ is profoundly decreased (~4-fold) to 2.9 ± 0.3 s^{-1} ($n = 6$) when $[Ca^{2+}]$ is reduced from pCa 4.6 to 8 in the continuous absence of ATP (Fig. 4 *A*). This indicates that rigor cross-bridges strongly slow down sTn switch-off kinetics, in contrast to the absence of their effect on switch-on kinetics.

DISCUSSION

We explored, to the best of our knowledge, for the first time the kinetics of Ca^{2+}-induced TnI switching inside contracting sarcomeres from fast skeletal muscle. Rapid mixing of Ca^{2+} with isolated sTn^{IAF} or sTn^{IAF} incorporated into the myofibrillar sarcomere induces biphasic fluorescence changes. Controls confirm that the biphasic kinetics originate from a single site, residue C133 on sTnI.

Interpretation of fluorescence phases

To determine the kinetics of the fast phase for isolated sTn ($k_{obs(fast)}{}^{+Ca}$ ~1000 s^{-1} at 10°C), we had to use a small μ-cuvette and a dead time of 0.25 ms. The typical dead time of ordinary cuvettes is ~2 ms. Within 2 ms, 86% of a fluorescence change with 1000 s^{-1} are lost. Following mixing of sTn.Tm.actin with 250 μM Ca^{2+} and a dead time of 4 ms, Miki detected monophasic kinetics with a k_{obs} of 530 ± 170 s^{-1} at 20°C (7). At similar $[Ca^{2+}]$ as used here (25 μM) and a dead time of 2 ms and at 4°C, Rosenfeld and Taylor obtained biphasic kinetics with $k_{obs(fast)}{}^{+Ca}$ ~500 s^{-1} for the isolated skeletal troponin C subunit, as well as for sTn.Tm.actin (3,8). Considering the uncertainties due to the dead time and the different temperature, the values of Rosenfeld and Taylor and ours are in good agreement. Thus, the similar kinetics of the fast fluorescence change in sTn^{IAF} observed here with isolated and sarcomeric sTn^{IAF} are most likely associated with the binding of Ca^{2+} to sTn with similar fast kinetics, as observed with troponin C alone (8).

Our transients obtained with selectively IAF-labeled sTn subunits and mapping of the IAF in sTnI peptides attribute the origin of the biphasic transients of sarcomeric sTn^{IAF} to a single site, C133 of sTnI. This agrees with the selective labeling of C133 after labeling the whole rabbit sTn with IANBD (25). C133 is located on a putative hinge of sTnI connecting the switch region (residues 116–131) (12) with the mobile C-terminal domain of sTnI (C-sTnI, residues 132–181). Our biphasic kinetics imply that Ca^{2+} induces a fast and a slow conformational change in sTnI. The fast change is most likely closely associated with Ca^{2+} binding to sTnC, not only due to its fast kinetics as observed with sTnC alone (8), but also because the fast phase is not observed in the study of Brenner and Chalovich (25). They triggered TnI switching by a mechanical protocol while keeping the $[Ca^{2+}]$ constant. The fast Ca^{2+}-induced change probed by IAF at C133 on sTnI in our study might therefore result from fast binding of the switch region to

the hydrophobic patch exposed in the N-lobe of sTnC when Ca^{2+} binds to sTnC (4,11,12).

C133 is in close proximity to the second actin-Tm binding region (residues 140–148) located on the mobile C-sTnI domain (34). Binding of C-sTnI to actin is stabilized by multiple electrostatic interactions allowing for multiple possible substates (13). The complete dissociation of the domain is therefore likely a slow process. Based on this biochemical and structural evidence, the slow fluorescence change probably reflects the slow dissociation of C-sTnI from actin.

Electron tomography of reconstituted thin filaments show that dissociation of C-sTnI from actin is required to enable Tm to move to a position on actin where it no longer blocks the acto-S1 interaction (15). The slow fluorescence change of sTn^{IAF} therefore probes a crucial process in thin filament activation/inactivation. This conclusion is corroborated by the similarity of our $k_{obs(slow)}{}^{+Ca}$-values with the k_{obs}-values of sTnI switching found by Brenner and Chalovich in skinned rabbit psoas fibers (25). At low [Ca^{2+}] our value obtained at 10°C is 21 s^{-1}, whereas their value at 4°C is 12 s^{-1}. At high [Ca^{2+}] our value is 150 s^{-1} and theirs is 60 s^{-1}. However, they also note that the time of mechanically induced cross-bridge detachment (5–10 ms) might limit their $sTnI^{NBD}$ kinetics at high [Ca^{2+}]. Because they induced $sTnI^{NBD}$ kinetics by releasing the feedback of cycling, force-generating cross-bridges on Tm, their $sTnI^{NBD}$ signal directly probes sTnI switching linked to Tm-based force regulation. Hence, the similar kinetics of our forward, slow Ca^{2+}-induced switch and their backward, Tm-induced switch of sTnI suggest that they both reflect the same regulatory switch of sTnI, i.e., the switch that transmits the Ca^{2+} signal from TnC to Tm to regulate the cross-bridge cycle.

Following dissociation of C-sTnI from actin, Tm can move to its on-position, which completes thin filament activation. The transitions among Tm-states in the presence of Ca^{2+} are fast (~400 s^{-1} at 10°C) (35) or even too fast to resolve its dynamics by stopped flow (36). This suggests that the dynamics intrinsic to Tm do not limit the rate of thin filament activation. Thus, sTnI switching likely represents the rate-limiting step in the thin filament activation and inactivation process.

Tn switching in solution and inside the sarcomere

Whereas the on-rate is only a little affected by in vitro reconstitution of sTn with Tm and actin to regulated thin filaments, the off-rate is strongly increased from 1.3 s^{-1} to 15–20 s^{-1} at 4°C (8). The ~8-fold increased off-rate after the sarcomeric incorporation of sTn^{IAF} observed in our study therefore likely results from the interaction of sTn with actin.Tm. These effects observed with sTnI are even stronger than the ones for cardiac TnC, where thin filament reconstitution increases the off-rate ~2.5-fold (17) and incorporation into myofibrils ~1.5-fold (19). This underlines the necessity for measuring the switch of sTnI in the sarcomere, especially for relating Tn kinetics to the kinetics of contraction and relaxation. Data from a recent study show that Ca^{2+} dissociates 8- to 10-fold more slowly from isolated sTn than the time taken for rabbit psoas myofibrils to relax (24). This unexpected finding can be explained by the faster switch-off of sarcomeric sTn compared to isolated sTn as found in our study.

Modeling of Ca^{2+}-dependent switch kinetics

The biphasic $sTnI^{IAF}$ transient provides evidence for a model with at least three states of sTnI. However, unlike our previous data with cTn incorporated into cardiac myofibrils (19), the dependence of fluorescence amplitudes on the [Ca^{2+}] with incorporated $sTnI^{IAF}$ cannot be simulated by a simple sequential model where the fast and the slow conformational change are direct consecutive transitions following Ca^{2+} binding (Fig. S3 *A*). Such a model results in loss of the fast phase when the speed of Ca^{2+} binding to sTnC (k_B[Ca^{2+}]) becomes slower than the forward transition k_{ON} of the slow regulatory change (Fig. S3 *D*). The intermediate state between the fast and slow change is then no longer significantly occupied. In fact, this is the case for cTn where the fast fluorescence change is lost at low [Ca^{2+}], i.e., at low Ca^{2+} activation when k_B[Ca^{2+}] < k_{ON} (19). However, to simulate the pronounced fluorescence decay observed at low [Ca^{2+}] (pCa $\geq$ 6.0) with sTn (e.g., Fig. 2 *D*, *light gray transient* or Fig. S1 *D, blue transient*), a second [Ca^{2+}]-dependent step needs to be inserted between the fast and slow fluorescence change (Fig. S3, *B* and E). On the basis of this idea, we designed a thermodynamically consistent model for sTn (Fig. S3, *C* and *F*) with the following properties: i), Ca^{2+} binding to each of the two regulatory sites of sTnC per se is limited by diffusion, and does not change fluorescence, ii), the fast conformational change of sTnI can already occur after binding of one Ca^{2+} to sTnC, and iii), Ca^{2+} binding to both regulatory sites on sTnC is required to trigger the slower conformational change of sTnI that regulates muscle contraction. The model can simulate the observed Ca^{2+} dependences (minimum and maximum values, pCa_{50} and *nH* values) of the rate constants and the fluorescence amplitudes of the two phases (Table S3).

Relation of switch-on and -off kinetics to kinetics of contraction and relaxation

An important question for skeletal muscle physiology is whether the rates of rise and decay of force are limited by the Ca^{2+}-controlled activation or inactivation of the thin filament. Brenner and Chalovich found mechanically induced switch kinetics of $sTnI^{NBD}$ to be ~15-fold faster than force redevelopment (25). This indicated that the regulatory system rapidly equilibrates compared to cross-bridge

turnover kinetics, and that the rate of force development is limited by cross-bridge turnover kinetics. Nevertheless, cross-bridge turnover kinetics are modulated by the Ca^{2+}-dependent shifts in the rapid equilibrium of Tn.Tm units, because not only steps in the cross-bridge cycle but also the fraction of switched-on Tn.Tm units determine the probability for transition of cross-bridge to the force-generating states. Our results validate these conclusions for Ca^{2+}-induced contractions. This perception is in line with time-resolved x-ray diffraction studies on intact muscles showing that the major changes in Tn-based meridional reflections occur at the onset of the twitch contraction, and only minor further changes occur when cross-bridges start to feed back on the Tm.Tn system (37).

Relaxation kinetics is biphasic with an initial slow, linear force decline (rate constant k_{LIN}) lasting for a time t_{LIN} while all sarcomeres remain isometric, followed by a ~10 times faster rapid exponential decay (rate constant k_{REL}) resulting from rapid lengthening, i.e., give, of sarcomeres (29). Mechanical studies indicate that k_{LIN} reveals the rate by which cross-bridges leave force-generating states under isometric conditions (28,29). Comparing k_{OFF} (~16 s^{-1}) obtained from stopped flow experiments with k_{LIN} (~2 s^{-1}) and k_{REL} (~21 s^{-1}) determined from force measurements indicates that sTnI switches off faster than cross-bridges detach during isometric relaxation, but not as fast as they detach during sarcomere give. Because in the stopped flow, myofibrils contract and relax unloaded, the true kinetics of the switch-off during loaded relaxation remains unclear from our study. However, the switch off is unlikely to be faster during loaded relaxation when more force-generating cross-bridges feed back through Tm on sTnI.

Therefore, a potential rate-limiting role for sTnI switching in the rapid phase of fast skeletal muscle relaxation clearly emerges from our results. This differs (8) from the situation for cardiac myofibrils, where k_{OFF} is ~10-fold higher than $k_{REL,}$ indicating that intrinsic kinetic properties of cTn per se do not rate-limit cardiac relaxation (19). The similar k_{OFF} and k_{REL} found here for rabbit psoas myofibrils are in line with findings from studies on rabbit psoas fibers, revealing that sTnC mutants with decreased Ca^{2+} dissociation slow down relaxation (23,24) whereas mutants with highly increased Ca^{2+} dissociation rates do not significantly change (23) or only slightly speed up (24) relaxation.

Strongly bound rigor cross-bridges prolonged the switch-off of sTnI fourfold, which is in agreement with fluorescence resonance energy transfer measurements on reconstituted thin filaments, showing that S1.ADP slows down switching of C-TnI and IR-TnI to actin (10). However, the slowing effect appears to be too strong to be meaningful for physiological muscle relaxation. Our value of $k_{obs(slow)}{}^{-Ca}$ measured under rigor conditions is sixfold smaller than the rate constant k_{REL} for myofibrillar relaxation in the presence of ATP, which would imply that relaxation can occur before, i.e., without the switch-off. Thus, it seems unlikely that rigor cross-bridges can mimic the effect of force-generating cross-bridges on thin filament inactivation. The feedback of cycling, force-generating cross-bridges on the Tm-Tn system might be weaker than that of strongly bound, noncycling myosin heads. Brenner and Chalovich concluded from their study that the feedback of force-generating cross-bridges is limited (25).

In conclusion, Ca^{2+} induces two conformational changes in sTnI as we have shown before for cTnC. However, there are also differences in the sTn and cTn mechanisms. Modeling of the data implies that both regulatory Ca^{2+} sites of sTnC must be occupied for the regulatory switch of sTnI to occur. Furthermore, the switch of sTnI not only determines the rates of thin filament activation and inactivation, but may also play a role in rate-limiting fast skeletal muscle relaxation. However, a limitation of our study is that in the stopped flow, myofibrils contract and relax in the absence of load. Using the sTnI switch assay with muscle preparations relaxing under load will enable us to elucidate the feedback of force-generating cross-bridges on thin filament inactivation.

SUPPORTING MATERIAL

Detailed methods, supporting results and modeling, and references (38,39) are available at http://www.biophysj.org/biophysj/supplemental/S0006-3495(12)00911-3.

The authors thank Stefan Müller and Franz-Georg Hanisch from the Centre for Molecular Medicine Cologne (CMMC) for the mass spectroscopy analysis.

This work was supported by grants from the CMMC (A6) and the Deutsche Forschungsgemeinschaft (SFB612-A2) to R.S. and G.P. and from the Medical Faculty of Cologne (Köln Fortune) to J.S. and R.S. A.L.-D. received a PhD fellowship from the Universidad de Costa Rica.

REFERENCES

1. Farah, C. S., and F. C. Reinach. 1995. The troponin complex and regulation of muscle contraction. *FASEB J.* 9:755–767.
2. Gordon, A. M., E. Homsher, and M. Regnier. 2000. Regulation of contraction in striated muscle. *Physiol. Rev.* 80:853–924.
3. Rosenfeld, S. S., and E. W. Taylor. 1985. Kinetic studies of calcium and magnesium binding to troponin C. *J. Biol. Chem.* 260:242–251.
4. Herzberg, O., J. Moult, and M. N. James. 1986. A model for the Ca^{2+}-induced conformational transition of troponin C. A trigger for muscle contraction. *J. Biol. Chem.* 261:2638–2644.
5. Dong, W., S. S. Rosenfeld, …, H. C. Cheung. 1996. Kinetic studies of calcium binding to the regulatory site of troponin C from cardiac muscle. *J. Biol. Chem.* 271:688–694.
6. Dong, W. J., C. K. Wang, …, H. C. Cheung. 1997. A kinetic model for the binding of Ca^{2+} to the regulatory site of troponin from cardiac muscle. *J. Biol. Chem.* 272:19229–19235.
7. Miki, M., and T. Iio. 1993. Kinetics of structural changes of reconstituted skeletal muscle thin filaments observed by fluorescence resonance energy transfer. *J. Biol. Chem.* 268:7101–7106.

8. Rosenfeld, S. S., and E. W. Taylor. 1985. Kinetic studies of calcium binding to regulatory complexes from skeletal muscle. *J. Biol. Chem.* 260:252–261.
9. Davis, J. P., and S. B. Tikunova. 2008. Ca^{2+} exchange with troponin C and cardiac muscle dynamics. *Cardiovasc. Res.* 77:619–626.
10. Xing, J., J. J. Jayasundar, …, W. J. Dong. 2009. Förster resonance energy transfer structural kinetic studies of cardiac thin filament deactivation. *J. Biol. Chem.* 284:16432–16441.
11. Takeda, S., A. Yamashita, …, Y. Maéda. 2003. Structure of the core domain of human cardiac troponin in the Ca^{2+}-saturated form. *Nature.* 424:35–41.
12. Vinogradova, M. V., D. B. Stone, …, R. J. Fletterick. 2005. Ca^{2+}-regulated structural changes in troponin. *Proc. Natl. Acad. Sci. USA.* 102:5038–5043.
13. Murakami, K., F. Yumoto, …, T. Wakabayashi. 2005. Structural basis for Ca^{2+}-regulated muscle relaxation at interaction sites of troponin with actin and tropomyosin. *J. Mol. Biol.* 352:178–201.
14. Pirani, A., M. V. Vinogradova, …, W. Lehman. 2006. An atomic model of the thin filament in the relaxed and Ca^{2+}-activated states. *J. Mol. Biol.* 357:707–717.
15. Galińska-Rakoczy, A., P. Engel, …, W. Lehman. 2008. Structural basis for the regulation of muscle contraction by troponin and tropomyosin. *J. Mol. Biol.* 379:929–935.
16. Li, M. X., L. Spyracopoulos, and B. D. Sykes. 1999. Binding of cardiac troponin-I147-163 induces a structural opening in human cardiac troponin-C. *Biochemistry.* 38:8289–8298.
17. Davis, J. P., C. Norman, …, S. B. Tikunova. 2007. Effects of thin and thick filament proteins on calcium binding and exchange with cardiac troponin C. *Biophys. J.* 92:3195–3206.
18. Bell, M. G., E. B. Lankford, …, R. J. Barsotti. 2006. Kinetics of cardiac thin-filament activation probed by fluorescence polarization of rhodamine-labeled troponin C in skinned guinea pig trabeculae. *Biophys. J.* 90:531–543.
19. Solzin, J., B. Iorga, …, R. Stehle. 2007. Kinetic mechanism of the Ca^{2+}-dependent switch-on and switch-off of cardiac troponin in myofibrils. *Biophys. J.* 93:3917–3931.
20. Stehle, R., and B. Iorga. 2010. Kinetics of cardiac sarcomeric processes and rate-limiting steps in contraction and relaxation. *J. Mol. Cell. Cardiol.* 48:843–850.
21. Gillis, T. E., D. A. Martyn, …, M. Regnier. 2007. Investigation of thin filament near-neighbour regulatory unit interactions during force development in skinned cardiac and skeletal muscle. *J. Physiol.* 580:561–576.
22. Little, S. C., S. B. Tikunova, …, J. P. Davis. 2011. Measurement of calcium dissociation rates from troponin C in rigor skeletal myofibrils. *Front Physiol.* 2:70.
23. Luo, Y., J. P. Davis, …, J. A. Rall. 2002. Determinants of relaxation rate in rabbit skinned skeletal muscle fibres. *J. Physiol.* 545:887–901.
24. Kreutziger, K. L., N. Piroddi, …, M. Regnier. 2008. Thin filament Ca^{2+} binding properties and regulatory unit interactions alter kinetics of tension development and relaxation in rabbit skeletal muscle. *J. Physiol.* 586:3683–3700.
25. Brenner, B., and J. M. Chalovich. 1999. Kinetics of thin filament activation probed by fluorescence of N-((2-(iodoacetoxy)ethyl)-N-methyl) amino-7-nitrobenz-2-oxa-1,3-diazole-labeled troponin I incorporated into skinned fibers of rabbit psoas muscle: implications for regulation of muscle contraction. *Biophys. J.* 77:2692–2708.
26. Trybus, K. M., and E. W. Taylor. 1980. Kinetic studies of the cooperative binding of subfragment 1 to regulated actin. *Proc. Natl. Acad. Sci. USA.* 77:7209–7213.
27. Brenner, B., T. Kraft, …, J. M. Chalovich. 1999. Thin filament activation probed by fluorescence of N-((2-(iodoacetoxy)ethyl)-N-methyl) amino-7-nitrobenz-2-oxa-1,3-diazole-labeled troponin I incorporated into skinned fibers of rabbit psoas muscle. *Biophys. J.* 77:2677–2691.
28. Tesi, C., N. Piroddi, …, C. Poggesi. 2002. Relaxation kinetics following sudden $Ca(^{2+})$ reduction in single myofibrils from skeletal muscle. *Biophys. J.* 83:2142–2151.
29. Stehle, R., M. Krüger, and G. Pfitzer. 2002. Force kinetics and individual sarcomere dynamics in cardiac myofibrils after rapid Ca^{2+} changes. *Biophys. J.* 83:2152–2161.
30. Greene, L. E. 1986. Cooperative binding of myosin subfragment one to regulated actin as measured by fluorescence changes of troponin I modified with different fluorophores. *J. Biol. Chem.* 261:1279–1285.
31. She, M., D. Trimble, …, J. M. Chalovich. 2000. Factors contributing to troponin exchange in myofibrils and in solution. *J. Muscle Res. Cell Motil.* 21:737–745.
32. Swartz, D. R., Z. Yang, …, J. P. Davis. 2006. Myofibrillar troponin exists in three states and there is signal transduction along skeletal myofibrillar thin filaments. *J. Mol. Biol.* 361:420–435.
33. de Tombe, P. P., A. Belus, …, C. Poggesi. 2007. Myofilament calcium sensitivity does not affect cross-bridge activation-relaxation kinetics. *Am. J. Physiol. Regul. Integr. Comp. Physiol.* 292:R1129–R1136.
34. Tripet, B., J. E. Van Eyk, and R. S. Hodges. 1997. Mapping of a second actin-tropomyosin and a second troponin C binding site within the C-terminus of troponin I, and their importance in the Ca^{2+}-dependent regulation of muscle contraction. *J. Mol. Biol.* 271:728–750.
35. Borrego-Diaz, E., and J. M. Chalovich. 2010. Kinetics of regulated actin transitions measured by probes on tropomyosin. *Biophys. J.* 98:2601–2609.
36. Maytum, R., S. S. Lehrer, and M. A. Geeves. 1999. Cooperativity and switching within the three-state model of muscle regulation. *Biochemistry.* 38:1102–1110.
37. Yagi, N. 2003. An x-ray diffraction study on early structural changes in skeletal muscle contraction. *Biophys. J.* 84:1093–1102.
38. Johnson, J. D., R. J. Nakkula, …, L. B. Smillie. 1994. Modulation of Ca^{2+} exchange with the Ca^{2+}-specific regulatory sites of troponin C. *J. Biol. Chem.* 269:8919–8923.
39. Robinson, J. M., H. C. Cheung, and W. Dong. 2008. The cardiac Ca^{2+}-sensitive regulatory switch, a system in dynamic equilibrium. *Biophys. J.* 95:4772–4789.